ELSEVIER

Biochimica et Biophysica Acta 1421 (1999) 249–260

BIOCHIMICA ET BIOPHYSICA ACTA
BBA

www.elsevier.com/locate/bba

Gadolinium induces domain and pore formation of human erythrocyte membrane: an atomic force microscopic study

Yi Cheng [a], Maozi Liu [b], Rongchang Li [a], Chen Wang [b], Chunli Bai [b], Kui Wang [a,*]

[a] *National Research Laboratories of Natural and Biomimetic Drugs, Beijing Medical University, Beijing 100083, People's Republic of China*
[b] *Institute of Chemistry, Chinese Academy of Sciences, Beijing 100080, People's Republic of China*

Received 31 March 1999; received in revised form 6 July 1999; accepted 22 July 1999

Abstract

Lanthanide cations bind to human erythrocyte membranes and enhance cell permeability. It was postulated that this effect is due to their likeness with calcium ions, which have been used to induce perforation of cells. However, the nature and mechanism of the perforation are still not clear. In the present work, the change in surface topography of erythrocyte membranes exposed to various gadolinium species was imaged with an atomic force microscope (AFM) in order to get direct evidence of perforation. The images of the whole cell and regions in nanometer scale showed that the normal surface is featured by closely packed nanometer size particles. The AFM images showed that Gd^{3+} binding to erythrocytes led to domain structure at low concentration and pore formation at higher concentration. The domain structures that appeared after incubation with 1.0×10^{-6}–1.0×10^{-5} mol/l Gd^{3+} solution for 30 min are featured by the particles aggregated to form ranges and the separations among them enlarged to gorges. With a higher concentration, 2.5×10^{-5} mol/l Gd^{3+}, the further aggregation developed into crater-shaped 'pores'. By washing with EDTA the 'pores' can be resealed but the domain structure remained. The anionic complex of Gd^{3+}, $[Gd(Cit)_2]^{3-}$ of this concentration, can only induce the domain structure formation. The domain and 'pore' structures mediated by Gd^{3+} concentrations might be responsible for both enhanced permeability and perforation. The mechanism of Gd-induced domain formation and perforation is discussed on the basis of aggregation of membrane proteins and the coexistence of different phases of membrane lipids resulting from Gd^{3+} binding.

Keywords: Gadolinium; Domain; Pore; Erythrocyte membrane; AFM

1. Introduction

Perforation of cell membranes is conceptually referred to enhanced permeability with the cell integrity unchanged. It can be accomplished by incubation with calcium chloride (~30 mmol/l) [1,2], in electric field pulse [3,4] or by lithotripter shock waves [5]. The calcium shock method has been used in gene recombination to increase the transformation rate of plasmid in bacteria [2]. In these cases, the perforation has been explained by Ca^{2+}-induced 'pore' formation, and pore formation has been used as the synonym of perforation. Although a few explanations for the perforation of cell membranes have been suggested [2–4], direct evidence of the perforation was required.

Recently, it was reported that the trivalent lanthanide cations, Ln^{3+}, can be used to increase the trans-

* Corresponding author. Fax: +86 (10) 62015584; E-mail: wangkui@mail.bjmu.edu.cn

0005-2736/99/$ – see front matter
PII: S0005-2736(99)00125-X

formation of plasmid in *Escherichia coli* as calcium chloride does, but in a lower concentration ($\backsim 10^{-5}$ mol/l) [6]. Yang et al. found a recoverable and sustainable hemoglobin-leaking phase during the attack of lanthanide ions on erythrocytes. They explain this effect on the basis of Ln^{3+}-induced perforation [7]. Other results related to the Ln^{3+}-enhanced permeability include that Tb^{3+} binding increases the uptake of the anticancer drug, cisplatin, by the ovarian cancer cells and La^{3+} binding stimulates Ca^{2+} influx in hepatocytes and thymocytes [8–10]. Recently, we found that the binding of Ln^{3+} to erythrocytes can facilitate the uptake of Ln^{3+} itself and other small molecules and ions [11–14]. Thus the Ln membrane systems could be used to study the nature of perforation.

The atomic force microscope (AFM) is the most prominent instrument among the scanning probe microscopes, which has been widely applied to investigate biological processes and topographic structures of the surface of living cells and biopolymers [15–20]. In earlier studies, the surface of erythrocytes has been imaged by AFM with both contact and tapping mode. By this means, the morphology of the whole erythrocyte was scanned at nanometer scale [21–23]. In the present work, we tried to scan the surface structure of the cell perforated by various concentrations of gadolinium ions, in order to observe the changes relating to perforation. The results revealed two different modes of perforation, the domain structure and the pore structure, depending on Gd^{3+} concentration. The results also support our previous suggestions that the Ln^{3+}-induced changes in membrane structure play a crucial role in the enhanced permeability of cells.

2. Materials and methods

2.1. Reagents and solutions

All the chemicals were of analytical grade unless stated otherwise. Gadolinium oxide (Gd_2O_3) and glutaraldehyde were purchased from Beijing Chemical Company. The stock solution of gadolinium chloride was prepared by dissolving the oxide in 5 mol/l HCl solution and heating to deplete the excess acid. The residue was diluted with Tris buffer (50 mmol/l, pH 7.4) to a certain volume. The Gd^{3+} concentration was determined by complexometric titration with xylenol orange as indicator. All the buffers (pH 7.4) used were prepared from Tris–HCl (A.R). The solution of gadolinium citrate, $[Gd(cit)_2]^{3-}$, was prepared by mixing the gadolinium chloride and sodium citrate solutions in a mole ratio Gd:Cit = 1:2 at pH 7.4.

2.2. Preparation of the specimens for AFM imaging

According to improved Butt's method [21], 1.0 ml of venous blood was obtained from the heart of a Wistar rat and anticoagulated with heparin–saline solution. The packed erythrocytes were separated by centrifuging at $2000\times g$ for 10 min and then washed with 310 mOsm Tris buffered saline (pH 7.4). Each 0.2 ml erythrocytes was incubated with gadolinium solutions in various concentrations which were diluted by Tris buffered saline (pH 7.4) at 35°C for 30 min. To prepare the samples for AFM imaging, the treated erythrocytes and the control were put into 1.5% glutaraldehyde in Tris buffer and stood for 3 min and rinsed with Tris buffer. The whole procedure was completed within 2 h. A 10 μl sample of the cell suspension was added to the freshly cleaved mica surface. The residual solution was removed with a piece of filter paper and air-dried.

2.3. AFM imaging

The AFM imaging was performed on a NanoScope III SPM (Digital Instruments, Santa Barbara, CA). The height (z) and lateral measurement (x,y) of the stage were calibrated with a 180 nm step height standard and a diffraction grating, respectively.

→

Fig. 1. Morphology of erythrocytes in the absence and presence of Gd species by AFM images. (A) Normal erythrocyte; (B) 1.0×10^{-6} mol/l Gd^{3+}-containing solution; (C) 2.5×10^{-5} mol/l Gd^{3+}-containing solution; (D) 1.0×10^{-5} mol/l Gd^{3+}-incubated erythrocyte treated by EDTA solution (5.0×10^{-3} mol/l EDTA, 150 mmol/l NaCl); (E) 7.5×10^{-5} mol/l Gd^{3+}-containing solution; (F) 2.5×10^{-5} mol/l $[Gd(Cit)_2]^{3-}$-containing solution.

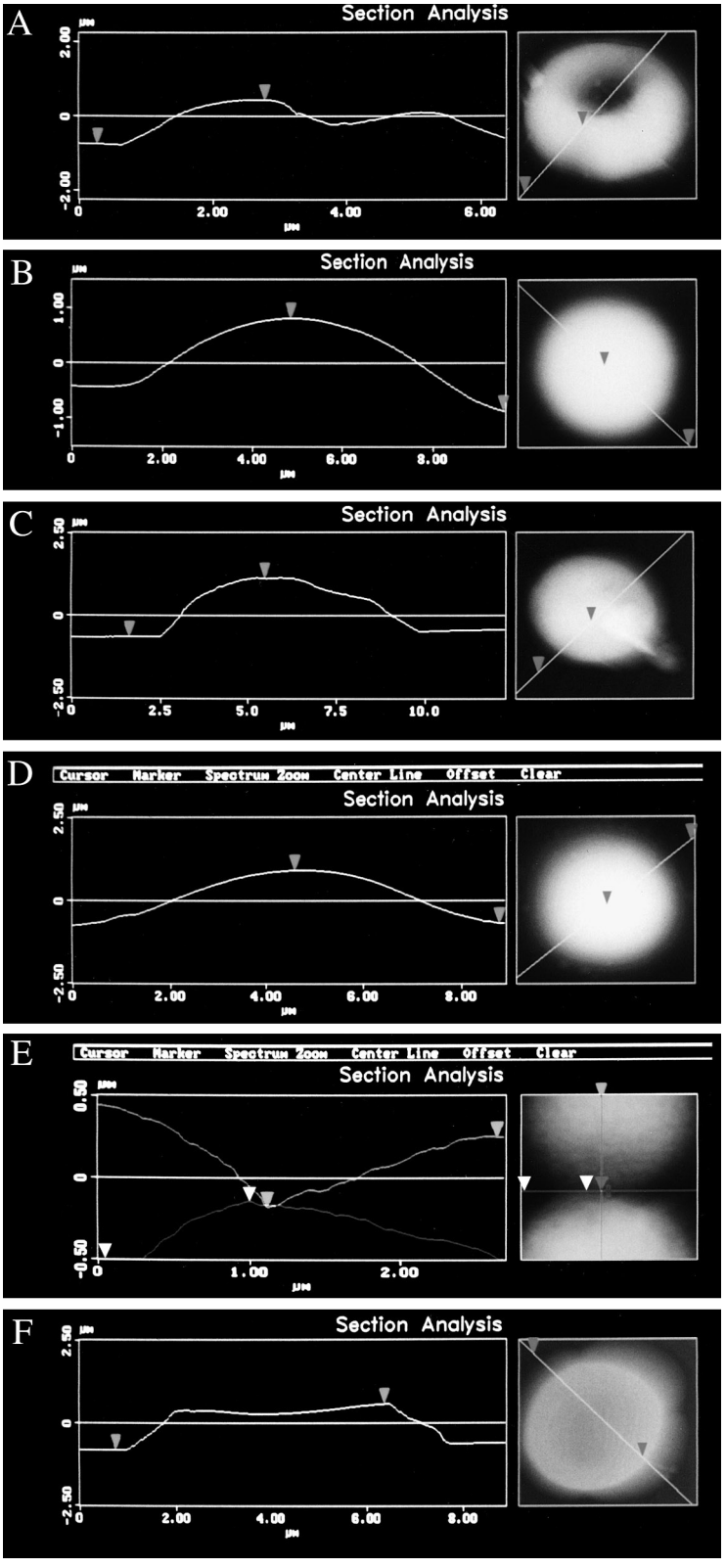
A
Section Analysis
2.00
0
-2.00
0
2.00
4.00
6.00
B
Section Analysis
1.00
0
-1.00
0
2.00
4.00
6.00
8.00
C
Section Analysis
2.50
0
-2.50
0
2.5
5.0
7.5
10.0
D
Cursor Marker Spectrum Zoom Center Line Offset Clear
Section Analysis
2.50
0
-2.50
0
2.00
4.00
6.00
8.00
E
Cursor Marker Spectrum Zoom Center Line Offset Clear
Section Analysis
0.50
0
-0.50
0
1.00
2.00
F
Section Analysis
2.50
0
-2.50
0
2.00
4.00
6.00
8.00

Commercially available tapping mode cantilevers were used (Digital Instruments). The cantilever was 125 μm long with a resonance frequency of about 313 kHz. The fixed erythrocytes were imaged on the AFM in the contact mode. Imaging forces were adjusted to less than 5 nN and all the AFM images were acquired in constant force mode.

3. Results

The results presented here indicate that both the cell shape and the membrane surface structure are sensitive to gadolinium and the effects are dependent on the species and concentrations of gadolinium.

3.1. The cell morphology

The AFM images of the whole erythrocyte, as shown in Fig. 1, revealed a remarkable difference in cell shape in the absence and presence of Gd^{3+} species. The intact erythrocytes display a typical doughnut shape with an average diameter of 5–8 μm and a maximal height in the peripheral region of about 1.25 μm (Fig. 1A). The incubation with Gd^{3+} caused cell swelling, characterized by the increased diameter and height of the central concave area (H_c) with increasing Gd^{3+} concentrations. A representative AFM image of a cell exposed to 1.0×10^{-6} mol/l gadolinium chloride is shown in Fig. 1B. The central region of the cells swelled to a convex surface with the H_c increased from an average 0.51 μm to 1.28 μm. With 5.0×10^{-6} mol/l Gd(III) chloride, H_c reaches 1.70 μm (image not shown). When the Gd(III) concentration was increased to 2.5×10^{-5} mol/l, H_c became 1.85 μm (Fig. 1C) and the pores of the cells appeared (details see Fig. 3C,D). An attempt to remove the surface bound gadolinium with EDTA could not turn the cells to their normal shape (H_c: 1.76 μm) and the size was still larger than that of the intact cells (Fig. 1D). A higher concentration (7.5×10^{-5} Gd^{3+} mol/l) resulted in cell fusion (Fig. 1E). With concentrations higher than 1.0×10^{-4} mol/l, irreversible hemolysis occurred and the erythrocytes collapsed. The cells incubated with 2.5×10^{-5} mol/l gadolinium citrate, though swollen, are somewhat concave (H_c: 1.11 μm) in shape (Fig. 1F). The statistical analysis of cell morphological changes as a function of Gd(III) concentrations in 100 μm^2 imaged range is given in Table 1.

3.2. Formation of domains and pores on the cell surface induced by gadolinium chloride

In order to gain insight into the fine structure of erythrocytes after exposure of cells to Gd species, we examined the local structure of the cell surface by zooming at several micro-regions of 500×500 nm^2. The AFM image of the surface of an intact erythrocyte is featured by closely packed globular particles with a diameter not larger than 50 nm (Fig. 2A). The contact regions among the neighboring particles appear as curved grooves with widths and a depths of only a few nanometers, as shown in a representative surface profile line (Fig. 2B). As pointed out in previous studies [21,22], the particles are the membrane proteins (peripheral and/or integral) protruding from the surface, while the lipid layer underneath was not observable. After incubation with low concentrations (1.0×10^{-6}–1.0×10^{-5} mol/l) of Gd(III) chloride for 30 min, the surface is characterized by a special 'domain' structure (Fig. 3A), in which the protein particles aggregated into ranges and the contact regions enlarged to gorges with an average width of 120 nm and depth of 4 nm (the contour scanned along the line on the surface is given in Fig. 3B). Underneath the gorges are the exposed regions of the lipid bi-

Table 1
Effect of gadolinium ions on erythrocyte shape (scan range: 100 μm^2)

Gd concentration (mol/l)	1.0×10^{-6}	5.0×10^{-6}	2.5×10^{-5}	7.5×10^{-5}	5.0×10^{-4}	2.5×10^{-5} (+EDTA)	$[Gd(Cit)_2]^{3-}$ (2.5×10^{-5})
Shape	Convex surface	Convex surface	Reversible hemolysis	Cell fusion	Irreversible hemolysis	Convex surface	Convex surface
Percentage of changed cells	73 ± 9%	90 ± 10%	75 ± 15%	80 ± 10%	90 ± 10%	85 ± 5%	75 ± 8%

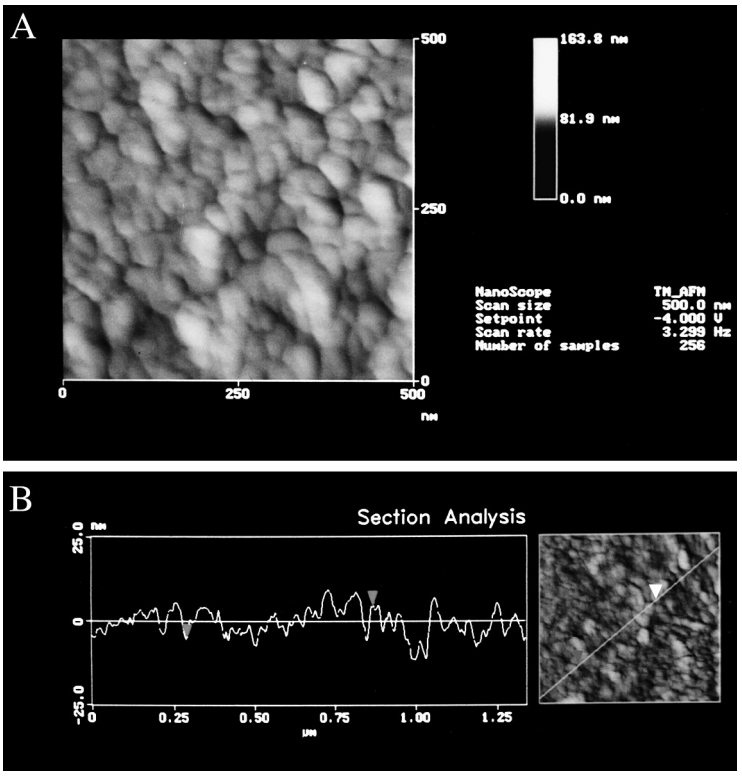

Fig. 2. AFM images of the fine structure in the surface of normal rat erythrocyte. (A) Scan sizes: 500×500 mm^2. (B) A representative surface contour along the line shown in the figure. This scan line defines the diameter and relative height or depth of the particles and curved groove-like structure.

layer. The number of domains in erythrocyte membrane exposed to 2.5×10^{-5} mol/l Gd(III) chloride is estimated to be $45 \pm 4/\mu m^2$ (see Table 2). When the erythrocytes were incubated with Gd(III) chloride of a higher concentration (2.5×10^{-5} mol/l), 'crater-like pores' were developed with approx. 4 pores/μm^2 (Fig. 3C, Table 2). The contours of these pores are characterized by a larger particle size (150–250 nm), pore depth ($\sim$ 73 nm) and diameter ($\sim$ 0.77 μm) (Fig. 3D,E and Table 2). As reported in our work [7], the cell membrane becomes permeable to intracellular proteins at this concentration, as characterized by the leaking out of hemoglobin. The AFM image in Fig. 3F shows the instant in which the intracellular macromolecules leaking out from the cell were fixed by glutaraldehyde and snapped. With the Gd concentration increased further to 5.0×10^{-5} mol/l, the membrane proteins aggregated to give larger particles and the width and depth of the gorges increased to expose the lipid bilayer further, but the crater-like pores were not observed (Fig. 3G). After incubation with 7.5×10^{-5} mol/l gadolinium chloride, the neighboring cells fused together due to intercellular aggregation of the protein particles, which are visible in the contacting region between the fused cells (Fig. 3H).

3.3. EDTA treatment removes the surface-bound Gd and reseals the pores

The protein aggregations might be affected by cross-linking via Gd^{3+} bridging or Gd^{3+} modulated conformational changes followed by association. These postulations were supported by the fact that the 'pores' on the surface of the erythrocytes perforated by 2.5×10^{-5} mol/l Gd(III) disappeared after EDTA washing (Fig. 4). As seen in the figure and the inserted contour, a domain structure similar to that observed in case of 1.0×10^{-6} mol/l Gd(III) chloride remained. Without the range-gorge feature, the domain structure (average 157/μm^2) is an array of many small depressions with an average 69 nm diameter and 4.6 nm depth (Table 2). The domain structure cannot be attributed to EDTA, since the control

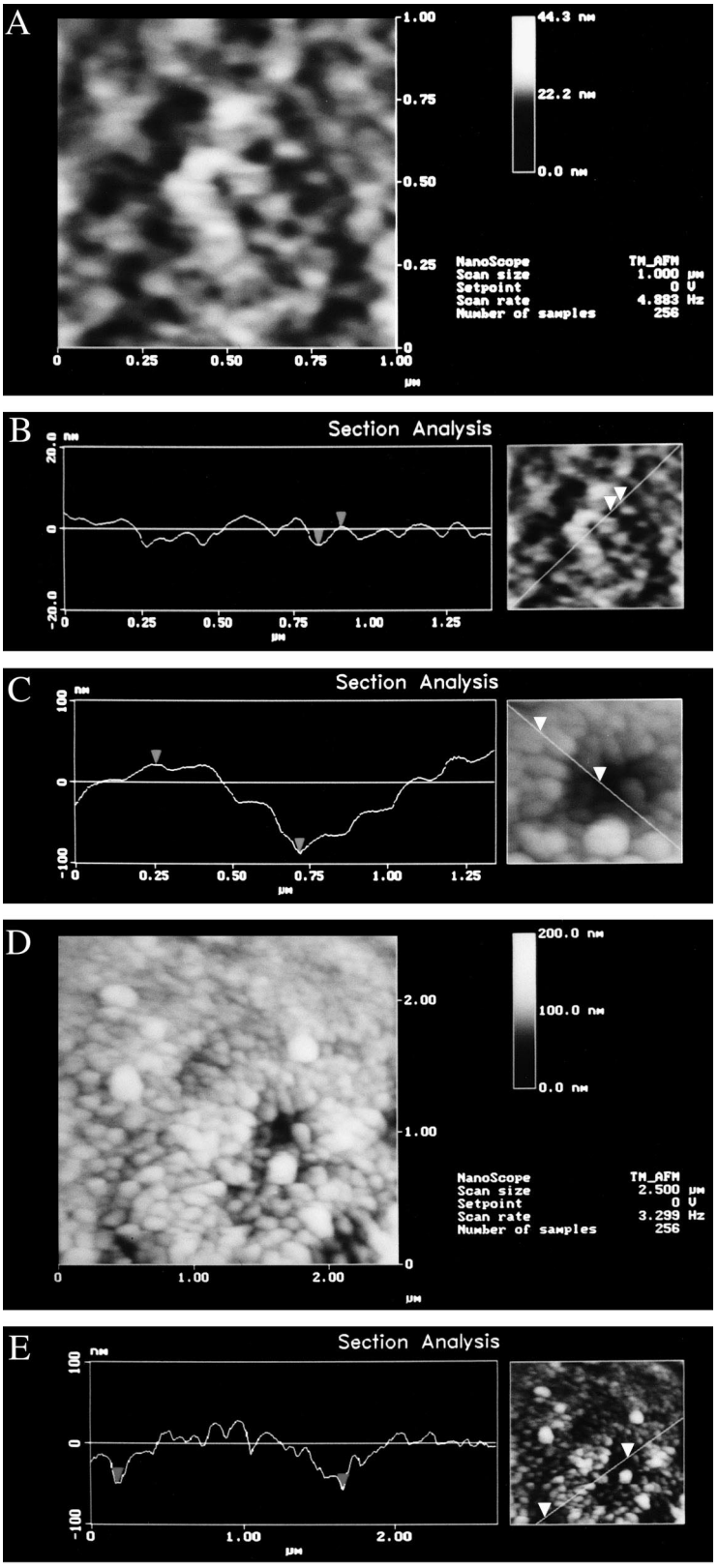
A
1.00
0.75
0.50
0.25
0
0.25
0.50
0.75
1.00
μm
44.3 nm
22.2 nm
0.0 nm
NanoScope
Scan size
Setpoint
Scan rate
Number of samples
TM_AFM
1.000 μm
0 V
4.883 Hz
256
B
Section Analysis
nm
20.0
0
-20.0
0
0.25
0.50
0.75
1.00
1.25
μm
C
Section Analysis
nm
100
0
-100
0
0.25
0.50
0.75
1.00
1.25
μm
D
200.0 nm
100.0 nm
0.0 nm
2.00
1.00
0
1.00
2.00
μm
NanoScope
Scan size
Setpoint
Scan rate
Number of samples
TM_AFM
2.500 μm
0 V
3.299 Hz
256
E
Section Analysis
nm
100
0
-100
0
1.00
2.00
μm

Fig. 3.

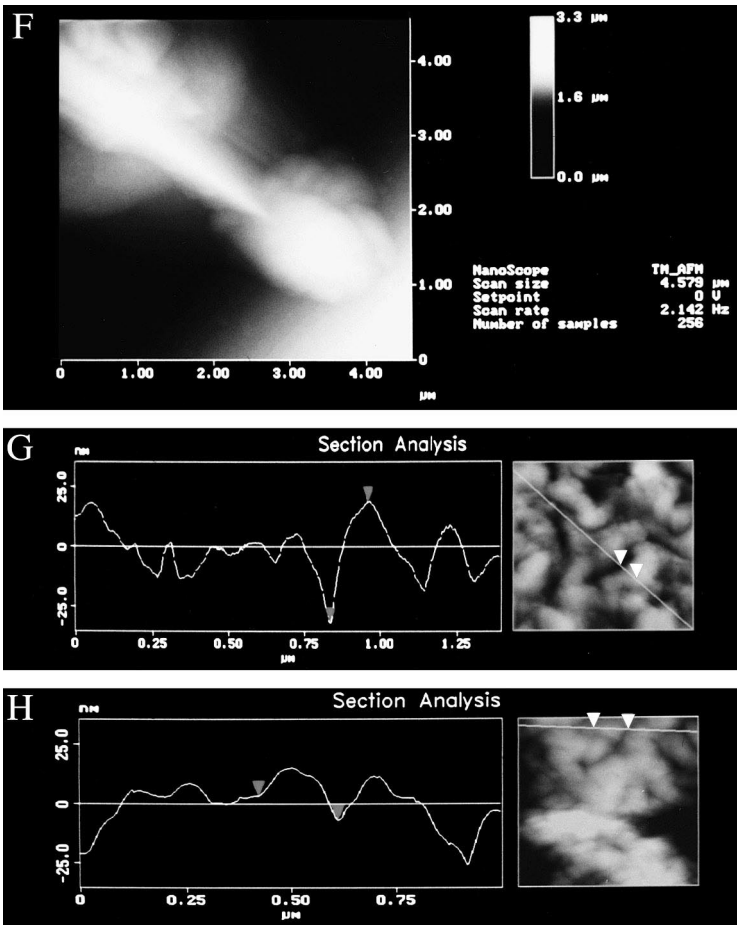

Fig. 3. AFM images of the domain structure and perforation in the surface of rat erythrocyte exposed to different Gd^{3+} concentrations. (A) 5.0×10^{-6} mol/l Gd^{3+} (scan sizes: 1.0×1.0 μm^2). (B) A representative surface contour along the line shown in the figure. This scan line defines the diameter and depth of the domain structure. (C) Representative surface contour of a pore along the line shown in the figure (the line defines the diameter and depth of the pore). 2.5×10^{-5} mol/l Gd^{3+}. (D) Representative local structure (scan sizes: 2.5×2.5 μm^2), 2.5×10^{-5} mol/l Gd^{3+}. (E) A representative surface contour along the line shown in the figure. This scan line defines the diameter and relative depth of the particles and pores. 2.5×10^{-5} mol/l Gd^{3+}. (F) The local image of erythrocyte leak (corresponding to Fig. 1C); scan sizes: 2.5×2.5 μm^2. (G) 5.0×10^{-5} mol/l Gd^{3+} (scan sizes: 1.0×1.0 μm^2). A representative contour line defines the aggregation extent of membrane proteins. (H) Two erythrocytes' fusion area (7.5×10^{-5} mol/l Gd^{3+}, scan sizes: 1.0×1.0 μm^2).

experiments showed that EDTA in the concentration used for washing cannot induce domain formation (image not shown here). Therefore, it demonstrates that gadolinium binding plays an important role in protein aggregation, while the 'pores' are resealed by removing the Gd^{3+}.

3.4. Gadolinium citrate induces domain structure only

The effect of Gd(III) citrate at a concentration of 2.5×10^{-5} mol/l on the surface structure is different from that of Gd(III) chloride at the same concentration. Only a more flattened range-gorge domain structure was observed (Fig. 5) with number and size close to those developed by 5.0×10^{-6} mol/l Gd(III) chloride (Table 2). No craters were formed when even higher concentrations of the citrate complex were used (images not shown). The results suggested that the free gadolinium ions are the active species for domain and pore formation and in the solution of the Gd complex, in which the concentration of free gadolinium ions is very low, only the domain structure was induced, as those observed after EDTA washing.

Table 2
Parameters of domain and pore structure induced by gadolinium (imaged erythrocyte number, $n = 3–5$)

	Number ± S.D. (/μm^2)	Diameter ± S.D. (μm)	Depth ± S.D. (nm)
Domain (Gd^{3+}: 5.0×10^{-6} mol/l)	45 ± 4	0.120 ± 0.03	4.0 ± 1.6
Domain ($[Gd(Cit)_2]^{3-}$: 2.5×10^{-6} mol/l)	41 ± 6	0.052 ± 0.06	4.5 ± 1.9
Domain (2.5×10^{-5} mol/l Gd^{3+}+EDTA)	157 ± 12	0.069 ± 0.04	4.6 ± 2.1
Pore (Gd^{3+}: 2.5×10^{-5} mol/l)	4 ± 1	0.771 ± 0.14	73.1 ± 6.8

In summary, when incubating with Gd^{3+} at low concentrations, Gd^{3+} binding to the cell surface causes swelling of the cells, but the integrity remains unchanged. At that time, the aggregation of the membrane proteins leads to a domain structure characterized by the range-gorge feature. The phospholipid layer in these regions is exposed and the permeability is enhanced. The size of the protein aggregates and the width of the exposed membrane lipids increase with increasing Gd^{3+} concentration. With higher Gd^{3+} concentrations, more extensive aggregations of the protein particles lead to the formation of crater-like pores and further increase in permeability, which is responsible for the reversible hemolysis. If the concentration is further increased, the Gd^{3+} binding results in cell fusion.

4. Discussion

4.1. On the present experimental method

In the present work, glutaraldehyde-fixed erythrocytes were imaged by AFM in contact mode under air-dried condition, as used in the previous studies [16,20–22]. As discussed in our previous work [20], glutaraldehyde fixation is an effective measure for the stabilization of erythrocytes. Fixation is necessary,

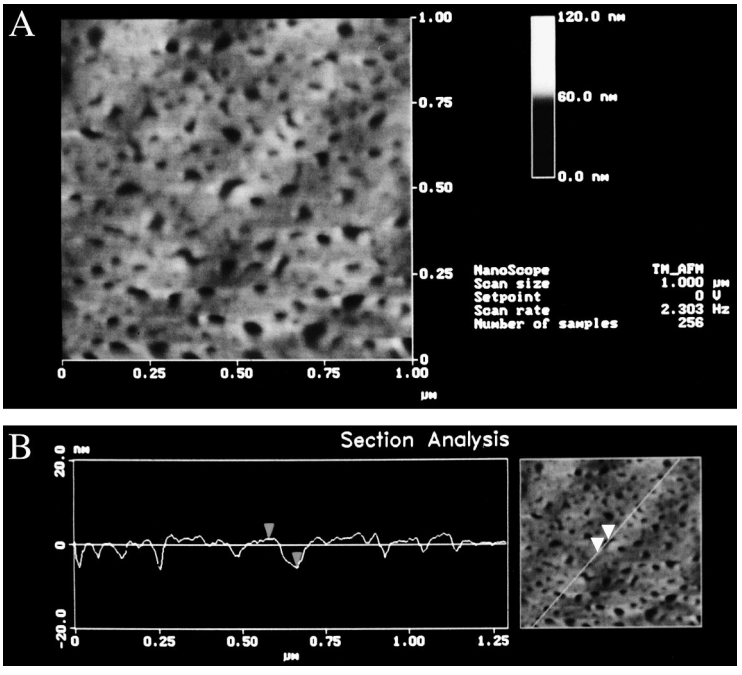

Fig. 4. AFM images of Gd^{3+}-incubated erythrocyte treated by EDTA solution. (A) Erythrocyte incubation with 2.5×10^{-5} mol/l Gd^{3+} for 30 min at 37°C, and then treated by EDTA solution (5.0×10^{-3} mol/l EDTA, 150 mmol/l NaCl). Scan sizes: 1.0×1.0 μm^2. (B) A representative surface contour along the line shown in the figure. The line defines the diameter and depth of the domain structure.

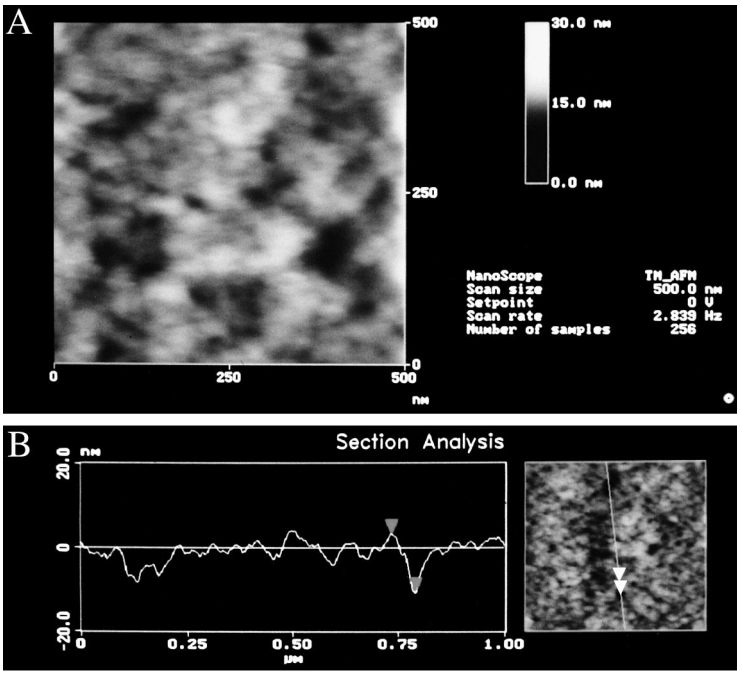

Fig. 5. AFM images of the domain structure in the surface of rat erythrocyte exposed to 2.5×10^{-5} mol/l $[Gd(Cit)_2]^{3-}$-containing solution. (A) Scan sizes: 500×500 μm^2. (B) A representative surface contour along the line in the local area of the surface of the erythrocyte. Note that this line defines the diameter and relative height or depth of the increased particles and depressions of domain structure.

because high-resolution images of cells are hardly achieved in solution. The softness of erythrocyte membranes and thermal fluctuation make the cells move and deform when the cells were tapped for scanning. It has been confirmed that the fixation does not alter the topographic features of the cell surface, though the particles observed might be slightly larger due to the expansion effect of glutaraldehyde, which induces some slight conformational changes of the proteins [22].

The attainable resolution of AFM studies on biological specimens depends strongly on the elasticity of the specimen [17,24], which is responsible for its softness. The membrane proteins have been shown to be much higher in elastic modulus ($\backsim 10^6$ Pa) than the membrane lipids [25]. Thus, up to now, AFM images can only exhibit the features of membrane proteins, while the head groups of phospholipids are 'invisible' [17]. Based on the previous studies [17,21–23], the particles on the erythrocyte surface presented here are clusters of the membrane proteins protruding from the membrane surface, including the peripheral and integral proteins. Underlying the depressions or the gorges among the protein particles there would be lipid layers exposed to the environment. The depth of a pore or a depression, as measured by stretching the tip into it, was just an estimated value, since the tip is of a pyramidal geometry and, in some cases, cannot access the bottom of a narrow depression. The development of finer cantilevers is critical to measuring the absolute depth of these depressions.

4.2. *Phase transition of lipid bilayer and aggregation of membrane proteins both contribute to gadolinium induced domain structure and pore formation*

It has been reported that, similar to Ca^{2+}, Ln^{3+} binding leads to domain formation in the lipid bilayer [26]. Unlike the Ln^{3+}-induced domain structure of cell membranes, the domain structure of phospholipid-only membranes was the result of phase transition, which led to the coexistence of two phases. It has been reported that lanthanide ions can induce H_{II} phase formation of phosphatidylethanolamine liposomes [27] and increase the transition temperature and decrease the membrane fluidity of dipalmi-

toylphosphatidylcholine liposomes [28]. Based on ^{31}P-NMR studies, we demonstrated that La^{3+} is also able to induce hexagonal (H_{II}) phase formation in the lipid bilayers of erythrocytes [13,29]. Phase transition would be considered one of the bases of domain formation. However, the present results indicate that the aggregation of membrane proteins might be more important in the formation of domain and pore structures. As shown previously [30], Gd^{3+} binding to membrane proteins such as spectrin leads to conformational changes and aggregations, but the aggregations in membranes are different from those in solution. Many extensive studies on protein aggregation in solution have been reported [31,32]. In these studies, the effect of the microenvironment on protein aggregation is negligible and the protein molecules move and impact freely and aggregate from many directions. On the other hand, aggregation of membrane proteins is limited to the neighboring molecules and confined by the membrane. [33]. These protein–protein and protein–lipid interactions limit the modes of aggregation and force the protein particles to form ranges, which are still in the lipid phase and restricted by the lipid phase. On the other hand, protein aggregation may also exert a force to make the array of lipid molecules become unevenly distributed and thus reinforce phase separation. However, limited by the relative amounts of proteins and lipids and confined by lipid-lipid interaction, the phase separation as well as the phase transition are limited to a number of small areas, i.e. the range-gorge pattern as imaged by AFM. Therefore, similar to the domain formation induced by electric field and diamides [34,35], the Gd^{3+} induced domain structures might be the overall results from three parts: (a) domains in the lipid bilayer, (b) lipid–protein domains at the interface between the lipids and intrinsic membrane-spanning proteins and (c) domains formed by protein aggregation.

Since EDTA can reseal the 'pore' and leave the domain structures on the surface, we can imagine that gadolinium ions bind mainly to the EDTA accessible sites. However, a fraction of gadolinium ions would be bound in the interior of the membrane. At low concentration (as in 1.0×10^{-6} mol/l), the gadolinium ions diffuse in and bind to the high affinity sites. According to Curmi et al. [36], the aggregation of membrane proteins induced by Ln^{3+} in a similar range of concentrations is reversible. Thus we can deduce that the protein aggregation induced by a very low concentration of Ln^{3+} is not extensive enough to cause pore formation. That is why only domain structure was observed with low concentrations of $GdCl_3$ and the citrate complex, as well as the protein-bound Gd^3 removed from the cell surface by EDTA treatment.

In summary, phase transition of the lipids and protein aggregation affect membrane structure and permeability cooperatively, though protein aggregation contributes very much to pore and domain development.

4.3. Domain and pore formation are related to enhanced permeability

Our previous studies revealed that Ln^{3+} binding enhances the transport of Ln^{3+} and the influx of small molecules as well as the outward leaking of hemoglobin from erythrocytes [11–14,29,37]. The leaking in of ascorbate, Ca^{2+} and Cl^- are determinable in concentrations as low as 10^{-6}–10^{-5} mol/l Gd^{3+}, while the leaking out of hemoglobin became determinable from 2.0×10^{-5} mol/l Gd^{3+}. In the former cases, influx via lipid domains was possible, as demonstrated in the Gd^{3+}-enhanced ascorbate influx [11]. As mentioned above, the AFM images indicate that Gd^{3+} binding to the erythrocyte membrane might result in the formation of three kinds of domains. Among them, the lipid domain structures due to local phase transition and phase separation have been known closely related to the permeability of cell membrane [34,35,38–40]. The domain structure can facilitate the passive permeation of small polar molecules across the membrane [38–41]. For the cell membrane, protein aggregation would reinforce and extend the domain structure in lipid bilayer to a 'range-gorge' form and increase the exposure of lipid bilayer. In addition, the permeability might also be enhanced by the 'mismatch' between lipids and peptide chains due to protein aggregation, since the molecular recognition between the lipid bilayer and membrane-spanning proteins is also important in the membrane architecture. It has been reported that the lipid–protein domains relating to the aggregation of proteins and the protein aggregate–lipid interaction give rise to the formation of aqueous

pores [34,35]. In addition, aggregates of intrinsic proteins might also form aqueous channels through the lipid bilayer, even though the walls of these channels would be constituted by a rather hydrophobic protein domain [35]. In model studies, the incorporation of integral membrane proteins into lipid vesicles composed of a single liquid crystalline species leads to considerable perforation [42,43]. After the treatment with Gd species, the whole shape of the erythrocyte displays cartouche, which is markedly different from the typical doughnut shape of the control (see Fig. 1). This is likely due to the fact that the influx of extracellular molecules, such as Ca^{2+}, Cl^{-} and other ions, results in an increase in intracellular osmotic pressure and then enhances the influx of water molecules.

In summary, the AFM images presented here support strongly the Ln^{3+} induced domain structures and pore formation, both of which increase the permeability of cell membranes. These effects are dependent on concentration and incubation time. It should be noteworthy that this perturbed structure with the increase in incubation concentration can further cause cell fusion and hemolysis.

Acknowledgements

This project was supported by the State Commission of Science and Technology and National Natural Science Foundation of China.

References

[1] M. Mandel, A. Higa, Calcium-dependent bacteriophage DNA infection, J. Mol. Biol. 53 (1970) 159–162.
[2] S.N. Cohen, A.C.T. Chang, L. Hsu, Nonchromosomal antibiotic resistance in bacteria: genetic transformation of *Escherichia coli* by R-factor DNA, Proc. Natl. Acad. Sci. USA 69 (1972) 2110–2114.
[3] D.S. Dimitrov, A.E. Sowers, Membrane electroporation-fast molecular exchange by electroosmosis, Biochim. Biophys. Acta 1022 (1990) 381–392.
[4] M.M.M. Henszen, M. Weske, S. Schwarz, C.W.M. Haest, B. Deuticke, Electric field pulses induce reversible shape transformation of human erythrocytes, Mol. Membr. Biol. 14 (1997) 195–204.
[5] S. Gambihler, M. Delius, J.W. Ellwart, Permeabilization of the plasma membrane of L1210 mouse leukemia cells using lithotripter shock waves, J. Membr. Biol. 141 (1994) 267–275.
[6] D.Y. Huang, S.J. Wu, D.I. He, Influence of yttrium chloride on transformation of plasmid PBR322. Chin. Biochem. J. (special issue of 8th National Symposium on Biochemistry and Molecular Biology) (1998) 231–232.
[7] X.D. Yang, X.T. Liu, B.W. Chen, R.C. Li, K. Wang, Hemolysis induced by the lanthanides and the entry of the lanthanides into erythrocyte, in: Proceedings of the First Sino-Dutch Workshop on the Environmental Behavior and Ecotoxicology of Rare Earth Elements, TNO-MEP, Delft, 1996, pp. 205–213.
[8] R.G. Canada, P.A. Andrews, K.M. Mack, A. Haider, The effects of terbium on the accumulation of cisplatin in human ovarian cancer cells, Biochim. Biophys. Acta 1267 (1995) 25–30.
[9] B.P. Hughes, S.E. Miton, G.J. Barritt, Effect of vasopressin and La^{3+} on plasma-membrane Ca^{2+} inflow and Ca^{2+} disposition in isolated hepatocytes, Biochem. J. 238 (1986) 793–800.
[10] J. Segal, Lanthanum increases the rat thymocytes cytoplasmic free calcium concentration by enhancing calcium influx, Biochim. Biophys. Acta 886 (1986) 267–271.
[11] Y. Cheng, B.W. Chen, J.F. Lu, K. Wang, The reaction of lanthanide ions with *n*-doxyl steric acids and its utilization for the ESR study on the permeability of lipid-bilayer of erythrocyte membrane to gadolinium ions, J. Inorg. Biochem. 69 (1998) 1–7.
[12] Y. Cheng, Y. Li, H. Yao, R.C. Li, K. Wang, Mechanism of gadolinium anion complex enters into human erythrocyte and its influence on chloride influx, J. Chin. Rare Earth 17 (1999) 54–59.
[13] Y. Cheng, H.Y. Yao, H.K. Lin, J.F. Lu, R.C. Li, K. Wang, The events relating to lanthanide ions enhanced permeability of human erythrocyte membrane: binding, conformational change, phase transition, perforation and ion transport, Chem.-Biol. Interact. 121 (1999) 267–289.
[14] Y. Cheng, Q.H. Huo, J.F. Lu, R.C. Li, K. Wang, The transport kinetics of lanthanide species in single erythrocyte probed by confocal laser scanning microscopy, J. Biol. Inorg. Chem. (1999) in press.
[15] R. Lal, S.A. John, Biological applications of atomic force microscopy, Am. J. Physiol. 266 (1994) C1–C21.
[16] M. Beckmann, H.A. Kolb, F. Lang, Atomic force microscopy of peritoneal macrophages after particle phagocytosis, J. Membr. Biol. 140 (1994) 197–204.
[17] J.M. Fernandez, Cellular and molecular mechanics by atomic force microscopy: capturing the exocytotic fusion pore in vivo?, Proc. Natl. Acad. Sci. USA 94 (1997) 9–10.
[18] C.A.J. Putman, K.O. van der Werf, B.G. de Grooth, N.F. van Hulst, J. Greve, Viscoelasticity of living cells allows high resolution imaging by tapping mode atomic force microscopy, Biophys. J. 67 (1994) 1749–1753.
[19] C. Perez-Terzic, J. Pyle, M. Jaconi, L. Stehno-Bittel, D.E. Clapham, Conformational states of the nuclear pore com-

plex induced by depletion of nuclear Ca^{2+} stores, Science 273 (1996) 1875–1977.
[20] H. Obserleithner, E. Brinckmann, A. Schwab, G. Krohne, Imaging nuclear pores of aldosterone-sensitive kidney cells by atomic force microscopy, Proc. Natl. Acad. Sci. USA 91 (1994) 9784–9788.
[21] H.J. Butt, E.K. Wolff, S.A.C. Gould, B.D. Northern, C.M. Peterson, P.K. Hansma, Imaging cells with the atomic force microscope, J. Struct. Biol. 105 (1990) 54–61.
[22] P.C. Zhang, C.L. Bai, Y.M. Huang, H. Zhao, Y. Fang, N.X. Wang, Q. Li, Atomic force microscopy study of fine structures of the entire surface of red blood cells, Scanning Microsc. 9 (1995) 981–988.
[23] M. Takeuchi, H. Miyamoto, Y. Sako, H. Komizu, A. Kusumi, Structure of the erythrocyte membrane skeleton as observed by atomic force microscopy, Biophys. J. 74 (1998) 2171–2183.
[24] M. Radmacher, M. Fritz, P.K. Hansma, Imaging soft samples with the atomic force microscope: gelatin in water and propanol, Biophys. J. 69 (1995) 264–270.
[25] V. Parpura, J.M. Fernandez, Atomic force microscopy study of the secretory granule lumen, Biophys. J. 71 (1996) 2356–2366.
[26] J. Seelig, R. Lehrmann, E. Terzi, Domain formation induced by lipid-ion and lipid-peptide interactions, Mol. Membr. Biol. 12 (1995) 51–57.
[27] F. Hwang, D. Zhao, J. Chen, X. Chen, J. Ni, Effect of lanthanum ions on the lipids polymorphism of phosphatidylethanolamines, Chem. Phys. Lipids 82 (1996) 73–77.
[28] X.M. Li, Y.F. Zhang, J.Z. Ni, J.W. Chen, F.H. Wang, The effect of lanthanide ions on the phase behavior of dipalmitoylphosphatidylcholine multilamellar liposomes, J. Inorg. Biochem. 53 (1994) 139–145.
[29] Y. Cheng, X.D. Yang, B.W. Chen, H.Y. Sun, R.C. Li, B. Zhu, J.Z. Ni, K. Wang, Cellular uptake and response to lanthanides, in: Proceedings of the Second Sino-Dutch Workshop on the Environmental Behaviour and Ecotoxicology of REEs and Heavy Metals, TNO-MEP, Delft, 1997, pp. 1–13.
[30] H.Y. Sun, H.K. Lin, Y. Gao, R.C. Li, R.D. Chen, K. Wang, Tb^{3+} binding to human erythrocyte spectrin resulting in conformation change and aggregation, J. Inorg. Biochem. 59 (1995) 29–37.
[31] L.R. De Young, A.L. Fink, K.A. Dill, Aggregation of globular proteins, Acc. Chem. Res. 26 (1993) 614–620.
[32] A.L. Fink, Protein aggregation: folding aggregates, inclusion bodies, Fold. Design 3 (1998) R9–R23.
[33] T. Gil, J.H. Ipsen, O.G. Mouritsen, M.C. Sabra, M.M. Sperotto, M.J. Zuckermann, Theoretical analysis of protein organization in lipid membranes, Biochim. Biophys. Acta 1376 (1998) 245–266.
[34] Y. Rosemberg, M. Rotenberg, R. Korenstein, Electroporation of the photosynthetic membrane: structural changes in protein and lipid-protein domain, Biophys. J. 67 (1994) 1060–1066.
[35] B. Deuticke, B. Poser, P. Lutkemeier, C.W. Haest, Formation of aqueous pores in the human erythrocyte membrane after oxidative cross-linking of spectrin by diamide, Biochim. Biophys. Acta 731 (1983) 196–210.
[36] P.M.G. Curmi, J.A. Barden, C.G. Dos Remedios, Conformational studies of G-actin containing bound lanthanide, Eur. J. Biochem. 122 (1982) 239–244.
[37] K. Wang, R.C. Li, Y. Cheng, B. Zhu, Lanthanide – the future drugs? Coord. Chem. Rev. 190–192 (1999) 297–308.
[38] W.L.C. Vaz, Percolation properties of two-component, two-phase phospholipid bilayers, Mol. Membr. Biol. 12 (1995) 39–43.
[39] S.G. Clerc, T.E. Thompson, Permeability of dimyristoyl phosphatidylcholine/dipalmitoyl phosphatidylcholine bilayer membranes with coexisting gel and liquid-crystalline phases, Biophys. J. 68 (1995) 2333–2341.
[40] L. Cruzeiro-Hansson, O.G. Mouritsen, Passive ion permeability of lipid membranes modelled via lipid-domain interfacial area, Biochim. Biophys. Acta 944 (1988) 63–72.
[41] M.A. Nesmeyanova, On the possible participation of acid phospholipids in the translocation of secreted proteins through the bacterial cytoplasmic membrane, FEBS Lett. 142 (1982) 189–193.
[42] A.T.M. Van der Steen, B. De Kruijff, J. De Gier, Glycophorin incorporation increases the bilayer permeability of large unilamellar vesicles in a lipid-dependent manner, Biochim. Biophys. Acta 691 (1982) 13–23.
[43] P. Van Hoogevest, A.P.M. Du Maine, B. De Kruijff, Characterization of the permeability increase induced by the incorporation of glycophorin in phosphatidylcholine vesicles: determination of the size of the non-specific permeation pathway, FEBS Lett. 157 (1983) 41–45.